IOP Conf. Series: Materials Science and Engineering **251** (2017) 012009 doi:10.1088/1757-899X/251/1/012009

Influence of fillers on the alkali activated chamotte

L Dembovska[1], G Bumanis[1], L Vitola[1] and D Bajare[1]

[1]Riga Technical University, Department of Building Materials and Products, Institute of Materials and Structures, Kalku str. 1, LV-1658, Riga, Latvia

E-mail: laura.dembovska@rtu.lv

Abstract. Alkali-activated materials (AAM) exhibit remarkable high-temperature resistance which makes them perspective materials for high-temperature applications, for instance as fire protecting and insulating materials in industrial furnaces. Series of experiments were carried out to develop optimum mix proportions of AAM based on chamotte with quartz sand (Q), olivine sand (OL) and firebrick sawing residues (K26) as fillers. Aluminium scrap recycling waste was considered as a pore forming agent and 6M NaOH alkali activation solution has been used. Lightweight porous AAM have been obtained with density in range from 600 to 880 kg/m^3 and compressive strength from 0.8 to 2.7 MPa. The XRD and high temperature optical microscopy was used to characterize the performance of AAM. The mechanical, physical and structural properties of the AAM were determined after the exposure to elevated temperatures at 800 and 1000°C. The results indicate that most promising results for AAM were with K26 filler where strength increase was observed while Q and OL filler reduced mechanical properties due to structure deterioration caused by expansive nature of selected filler.

1. Introduction

The alkali activated materials (AAM) can ensure performance comparable to traditional cementitious binders in a wide range of applications and with the added advantage of significantly reduced Greenhouse emissions [1]. Since the AAM are aluminosilicate based mineral materials they could be expected to be used as refractory materials [2],[3]. However, co-existance of alkali components in the AAM at high temperatures decrease the physicochemical properties of the refractories due to the formation of compounds with lower melting points [4]. The range of thermal applications brings different thermal load demands to the AAM products. Refractory insulating products are generally exposed to gradual heating rates and long periods at high temperature, whilst fire resistant products are designed to be exposed to fast initial temperature increases for a relatively short duration [5]. In order to optimise thermal properties, the control of thermal expansion and retention / development of physical properties during elevated temperature exposure is desirable. The use of thermally stable (filling) materials to minimise thermal expansion / shrinkage is common in other materials technologies. Kamesu et al. made potassium activated metakaolin geopolymers filled with fine quartz (100µm – 1mm) or α-alumina (0.1-100µm) to evaluate thermal properties of the blends [6]. The maximum shrinkage of the control geopolymer was 17% at 1000°C which was reduced to 12% by adding alumina and to 13% by adding quartz. The temperature of maximum densification shifted from 1000°C in the control sample to 1150°C and 1200°C, respectively by adding 75 wt. % α-quartz and alumina.

The aim of this research was to obtain the chamotte based AAM with low shrinkage in temperatures up to 1000°C. The firebrick sawing by-products, quartz and olivine sand were evaluated as thermally

stable fillers. Aluminium scrap recycling waste was used as pore forming agent to obtain the lightweight AAM with heat resistance of up to 1000°C for industrial use.

2. Materials and test methods

2.1. Raw materials

Except for chamotte and quartz sand the other selected raw materials were ground for 30 min with speed of 300 rpm in the laboratory planetary ball mill Retsch PM 400 to obtain powder raw material. Chemical composition of raw materials is presented in table 1. Grading analysis of raw materials is given in figure 1, except for aluminium scrap recycling waste due to its reactive nature [7].

Table 1. Chemical composition of raw materials (wt.%).

Chemical component	ASRW	CH	K26	Q	OL
Al_2O_3	63.2	18.8	58	1.4	0.8
SiO_2	7.9	76.7	39.1	96.8	42.1
CaO	2.6	0.3	0.1	-	-
SO_3	0.4	-	-	-	-
TiO_2	0.5	1.2	0.1	-	-
MgO	4.4	0.5	0.2	-	49.3
Fe_2O_3	4.5	0.7	0.7	0.3	-
$Na_2O+ K_2O$	7.7	1.8	1.7	-	0.1
Other	2.6	-	-	0.5	-

Chamotte (CH) used in the research is commercial material from Ltd. 'Witgert'. The median particle size of CH was 126 μm (figure 1). According to the XRD analyse chamotte contains the following minerals: cristobalite (SiO_2), quartz (SiO_2) and mullite ($Al_6Si_2O_{13}$).

Aluminium scrap recycling waste (ASRW) is the final waste product at the aluminium scrap recycling factories. Chemical composition is given in table 1. Main oxides are Al_2O_3 (63.2 wt.%), SiO_2 (7.9 wt.%), CaO (2.6 wt.%) and Na_2O+K_2O (7.7 wt.%). According to the XRD analysis, the ASRW contains metallic aluminium (Al), iron sulphite ($FeSO_3$), aluminium nitride (AlN), aluminium iron oxide ($FeAlO_3$), magnesium dialuminium ($MgAl_2O_4$), α-quartz, aluminium chloride ($AlCl_3$) and aluminium hydroxide ($Al(OH)_3$). Ground ASRW with fraction <1 mm was used as the pore forming agent.

Firebricks sawing residues (K26) (produced by Ltd. 'Morgan Thermal Ceramics') could be classified as a by-product from the sawing process of furnace production. The K26 is aluminosilicate material and its chemical composition is presented in table 1. The median particle size was 3.5 μm (figure 1). According to technical data sheet working temperatures of the K26 is range from 1260°C to 1790°C. The K26 are made from high-purity refractory clay with high amount of Al_2O_3. The XRD analysis indicates mullite ($Al_6Si_2O_{13}$) and aluminium oxide or curundum (Al_2O_3).

Quartz sand (Q) (produced by Ltd. 'Saulkalne S') was used as locally available natural filler (< 0.3 mm). Median particle size was 126 μm (figure 1). The mineralogical composition of Q was α-quartz.

Olivine sand (OL) is natural olivine sand from Norway (size 0.3 – 2 mm). The median particle size was 192 μm (figure 1). The XRD analysis indicate such minerals as forsterite ($Mg_2(SiO_4)$), ringwoodite ($(Mg,Fe)_2SiO_4$). Chemical composition is presented in table 1 and main oxides are MgO (49.3 wt.%) and SiO_2 (42.1 wt.%).

Sodium hydroxide solution – the 6M NaOH alkali activation solution was prepared of the commercially available sodium hydroxide flakes from Ltd. 'Tianye Chemicals' (China) of 99% purity.

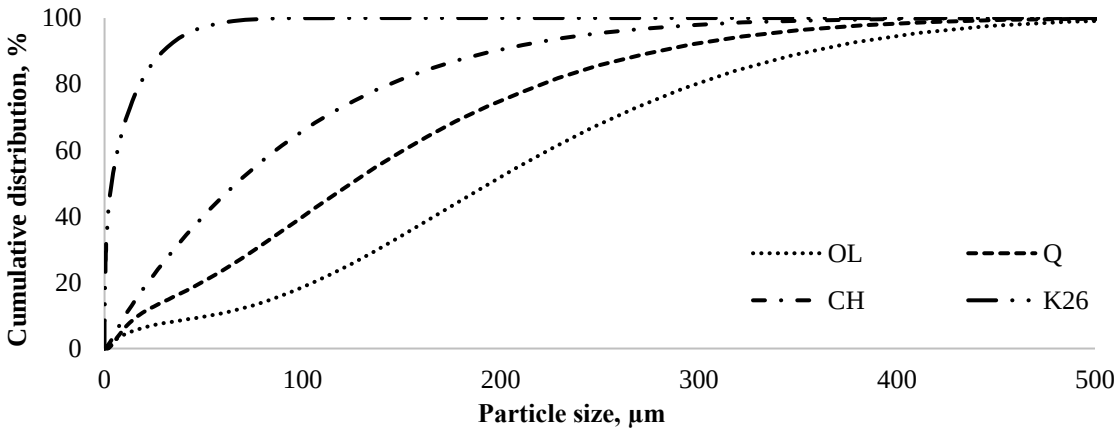

Figure 1. Particle size distribution of raw materials: OL – olivine sand, Q – quartz sand; CH – chamotte; K26 - firebricks sawing residues.

2.2. Sample preparation and curing conditions

The AAM were prepared by mixing the CH precursor with selected fillers (K26, OL or Q) according to mixture composition given in table 2. All the ingredients were cooled down to -21°C before mixing. Sodium hydroxide solution was added to blend of dry ingredients and mortars were mixed for 1 minute. Subsequently, the AAM were cast into moulds with size of 40x40x160mm and then vibrated on a vibration table for 5 sec. The moulds were covered with plastic films and specimens after limited pore structure formation were cured in 80°C for 24h. Then the samples were kept in a room temperature before their exposure to high temperature of 800°C and 1000°C.

Table 2. Alkali activated material compositions - dry ingredient ratios (wt.%).

	S	0.3K	0.5K	0.3Q	0.5Q	0.3OL	0.5OL
ASRW	10	10	10	10	10	10	10
CH	100	70	50	70	50	70	50
K26	-	30	50	-	-	-	-
Q	-	-	-	30	50	-	-
OL	-	-	-	-	-	30	50
6M NaOH			33% from all dry components				

2.3. Test methods

Chemical composition of dry raw materials were determined according to the LVS EN 196-2 with precision +/- 0.5%. Particle size distribution in powder materials was determined by the Analysette 22 Nano Tec laser granulometer. Specific surface area was detected by the BET method ('Nova 1200 E-Series, Quantachrome Instruments'). Effective diameter was detected by the Zeta potential ('90 Plus' and 'MAS Zeta PALS Brookhaven Instr'). To determine the mineralogical composition of raw materials and AAM before and after heat treatments the X-ray diffraction (XRD) patterns of the powdered samples were recorded on a "RIGAKU ULTIMA+" diffractometer using CuKα radiation, the test were run in a 2-Theta range of 5 - 70º. Physical properties of the AAM, such as bulk density and water absorption were determined in accordance with the EN 1097-6 and the EN 1097-7, the open porosity was determined by water absorption taking into account the volume of the prepared specimens. Bending and compressive strength of the hardened AAM was tested according to the LVS EN 196-1 at the age of 28 days. The AAM microstructure was observed by using scanning electron microscope ('TESCAN Mira / LMU Field-Emission-Gun'). High temperature microscopy (HTOM) EM201, HT163 was used to determinate heat resistance and shrinkage of the AAM in temperatures up to 1400°C. Samples have been tested by heating rate 80°C/min up to 500°C temperature and then switched to 15ºC/min while reaching 1400°C temperature.

3. Results and discussion

3.1. XRD results

The heat treatment impact on material minerology was studied by X-ray diffraction. In figure 2 is shown the impact of heat treatment at 800, 1000 and 1200°C on mineralogical enhancement of alkali activated mixture of chamotte and firebrick sawing residues (mixture 0.5K). The shift to higher degrees of halo at 2-Theta = 10 - 30° that presents amorphous phase in raw materials is characterized as N-A-S-H gel formation during alkali activation process [8].

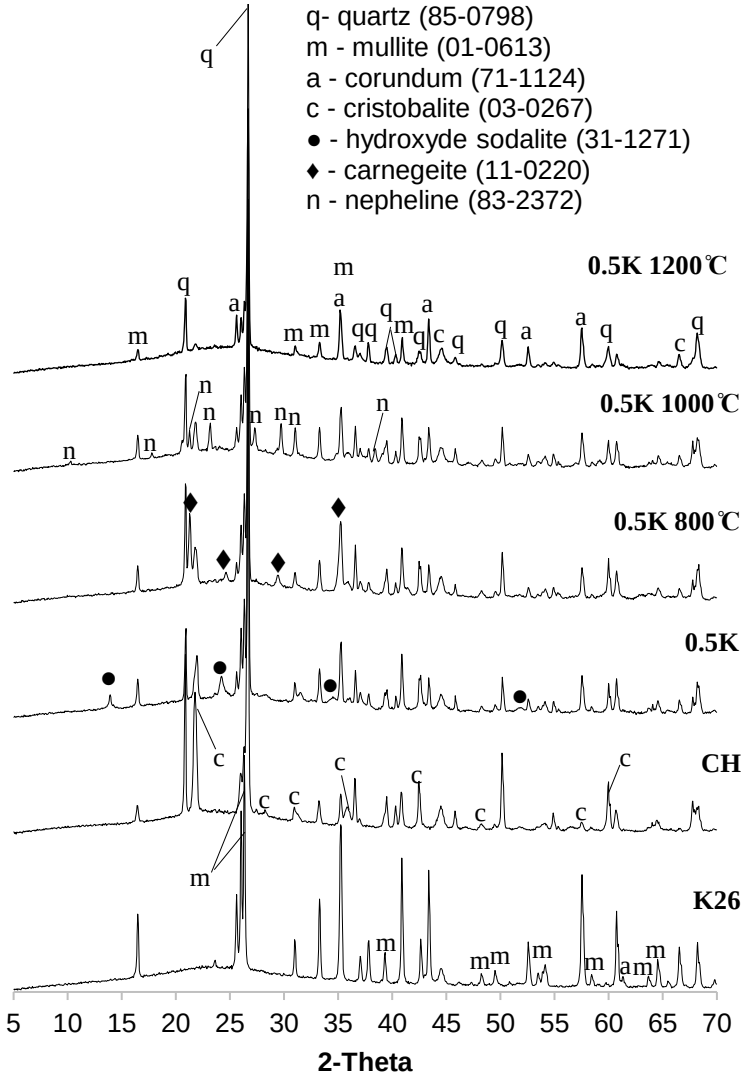

Figure 2. XRD analysis of raw materials CH, K26 and AAM 0.5K before and after heat treatment.

Prepared AAM 0.5K has some crystalline phases which come from raw CH and K26 like mullite ($Al_{4.56}Si_{1.44}O_{9.72}$), quartz ($SiO_2$), corundum ($Al_2O_3$) and cristobalite ($SiO_2$). Hydroxide sodalitie ($1.08Na_2O{\cdot}Al_2O_3{\cdot}1.68SiO_2{\cdot}1.8H_2O$; sodalite group zeolites) and N-A-S-H gel which form during the activation process of CH also are detected. Considerable N-A-S-H gel changes after heat treatment at different temperatures have not been detected by X-ray diffraction. Meanwhile after heat treatment at 800°C the hydroxide sodalite has not been detected, but new crystalline phase called carnegeite ($NaAlSiO_4$) was indicated. That could be explained by hydroxide sodalite tranformation into zeolite X, which melts at 760°C and becomes amorphous; and at 800°C recrystallizes again as carnegeite [9]. After

heating at 1000°C such phases as quartz, mullite, corundum and cristobalite remained and new crystalline phase - nepheline ($Na_{6.65}Al_{6.24}Si_{9.76}O_{32}$) was detected. Nepheline transforms from carnegeite at the temperature around 900°C-1000°C. At the 1200°C the previously determined corundum, mullite and cristobalite as well as quartz were detected with lower intensity, but other crystalline phases are disappeared, that could be explained by zeolite crystal melting and transforming into amorphous phase at 1150ºC [9].

3.2. Physical properties

The material bulk densities have been determined for samples (initially cured at 80°C) and after their exposure to 800°C and 1000°C temperature. Results are presented in figure 3. The obtained AAM are highly porous and a typical microphotograph taken by the SEM is presented in figure 4. There is not significant difference between SEM microphotographs taken of AMM with different composition. Variety of the AAM densities can be influenced by two factors – the increase of particle size of the filler materials (a): the OL with coarser particle size has the highest density, while finer particles (Q, K26) ensure lower density; or the change of fresh paste workability and viscosity (b) – larger particles ensure paste with lower viscosity (equal amount of activizator was used for all compostion) releasing gas produced during the pore forming process. Most probably the density of the AAM after its high temperature exposure slightly decreased due to changes of AAM` s crystalline phases. Some correlations can be observed comparing the water absorption and material density (figure 3 and figure 5). The open porosity (figure 6) was in range of 24 to 32 vol%.

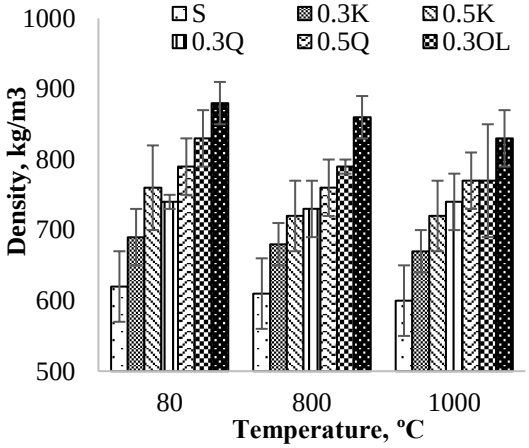

Figure 3. Bulk density of AAM with fillers

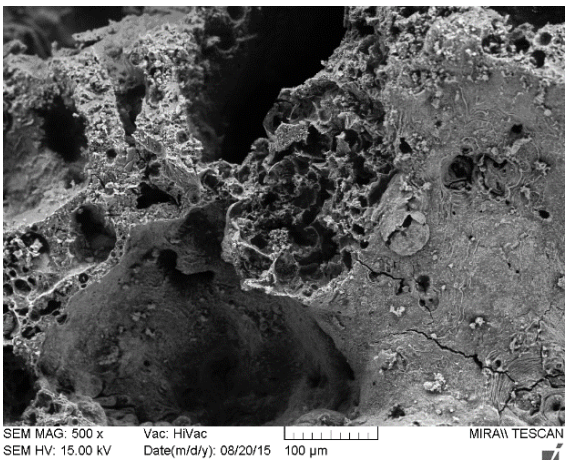

Figure 4. SEM microphotograph of 0.3Q.

The water absorption by mass % is given in figure 5. Sample S had the lowest density (600-620 kg/m^3) and it resulted in the water absorbtion in the range of 37.9-48.2%. In comparison, 0.5OL had the highest density of all AAM (830-880 kg/m^3) and 0.5OL had water absorption results in the range of 26.1-28.2%. The high temperature treatment (800 and 1000ºC) has changed open porosity and there were two correlations observed: 1) the high temperature treatment reduced open porosity (the samples with index S – from 31.2 to 27.2 and 23.7 vol.%; K – 0.5K from 33.4 to 31.3 and 30.9 vol.%) (figure 6), which could be attributed to the fact that the open pores had been partially filled with products having melting point under 1000ºC (figure 6); glasification and densification of pores' walls and material internal structure occurred; 2) the high temperature treatment increased open porosity (the samples with Q – for 0.5Q from 29.3 to 27.7 and 29.4 vol.%; OL – for 0.3OL from 29.9 to 24.1 and 29.4 vol.%) (figure 6), which could be linked to polymorph transition of the filler provided with filler expansion leading to the cracks and the structure becoming more open porous (figure 4).

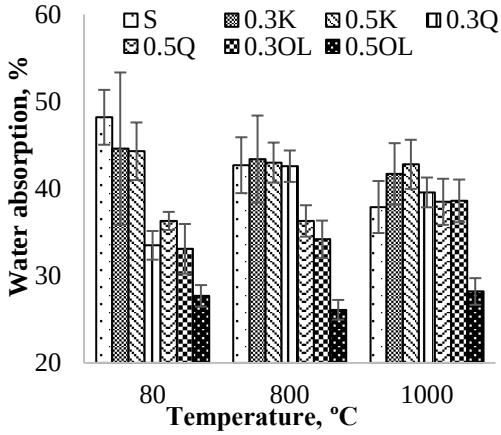

Figure 5. Water absorption (mass %) of AAM.

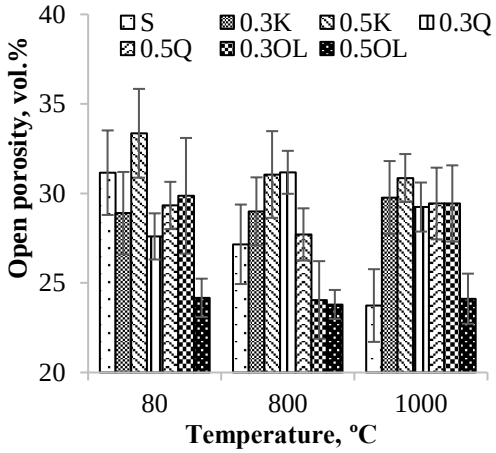

Figure 6. Open porosity vol. % for AAM.

3.3 Mechanical properties

The obtained mechanical properties of the AAM were affected by the mixture composition and the material physical properties. The mechanical strength was influenced by the pore structure, determined by the fineness of raw materials. The initial compressive strength of the AAM was from 0.8-2.0 MPa, the highest strength was for the compositions with K26 filler (finest filler), the lowest – with OL filler (coarser filler). Obviously coarser filler grains transmit stresses with lower efficiency notwithstanding their higher density [10].

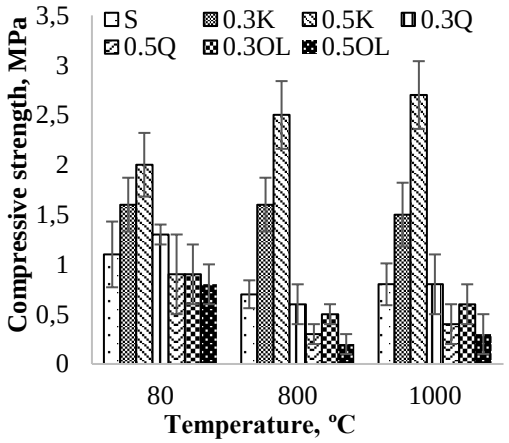

Figure 7. Compressive strength test results.

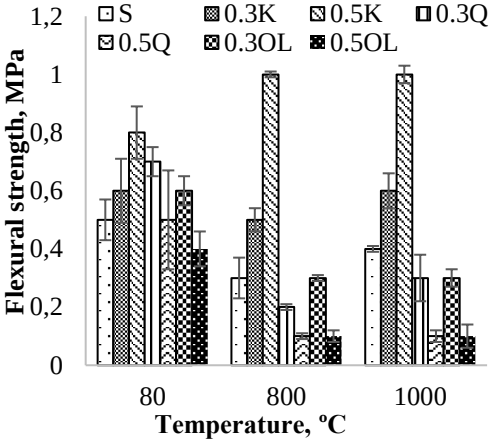

Figure 8. Flexural strength test results.

The AAM exposure to high temperature treatment (800 and 1000°C) changed the mechanical properties significantly. In most compositions the compressive strength decreased: 1.1 to 0.7 and 0.8 MPa (mixture S), 1.3 to 0.6 MPa (0.3Q), 0.9 to 0.3 MPa (0.5Q), 0.9 to 0.2-0.5 MPa for the AAM with OL. The decrease of strength can be described by phase change transition for filler materials (Q and OL) where polymorph changes occurred causing volume change of filler materials and thus damaging the inner structure of the material, these observations were also associated with changes of physical properties described in section 3.2. Meanwhile in the samples with K26 filler there was an increase in compressive strength. The K26 is a refractory material by its nature; therefore it was stable in the structure of AAM and even increased the compressive strength after exposure to 1000°C from 1.9 to 2.7 MPa for 0.5K. Mechanical properties for AAM is strongly affected by Al content in compositions (table 1). In case of composition 0.5K this may be one of the decisive factors. For Q and OL compositions Al content is low. Similar tendencies were detected from flexural strength results (figure 8). After heat treatment and thermal deformations the microcracks occurred in the structure of AAM thus significantly reducing the flexural strength. The only composition indicating flexural strength increase was the one

with K26 filler – 0.8 to 1.0 MPa. The flexural strength was reduced to 0.1-0.4 MPa in the rest of compositions.

3.4. High temperature microscopy

High temperature microscopy results can be divided relatively in three intervals: (a) area changes in up to 750°C; (b) 750 to 850°C and (c) 850 to 1000°C (figure 9). Within up to 760°C the expansion was observed with maximal intensity at 600°C: 1.9% for 0.5Q, 1.2% for 0.5OL, 2.9% for 0.5K and 1.4% for S. Thermal expansion results can be influenced by the porous structure of AAM therefore expansion can occur inside the pores and the true expansion value could be even greater. Shinkage in the temperature interval from 750-850ºC can be attributed to the zeolite crystal melting and transformation processes to other minerals. As mentioned in section 3.1. at 760ºC zeolite X melts and changes its phase to amorphous [9], but at 800ºC it recristalyzes and transforms into carnegeite.

According to table 3 at 750°C material 0.5Q reached 101.5% of the area, 0.5OL – 100.8%, 0.5K – 100.3% and S – 101.2%. At 850°C all AAM started to shrink – materials reached total area of 97.8% for 0.5Q, 97.6% – 0.5OL, 96.4% for 0.5K and 97.7% for S. At 1000°C material shrinkage reached approximately 4% for all AAM (table 3).

Table 3. Shrinkage of the AAM at described temperatures.

Temperature, °C	0.5Q Area, %	0.5OL Area, %	0.5K Area, %	S Area, %
750°C	101.5	100.8	100.3	101.2
850°C	97.8	97.6	96.4	97.7
1000°C	96	97.2	95.7	96

The obtained results are rather similar, and it was concluded that fillers (quartz, olivine sand and K26) used in this study have no significant influence on the material shrinkage in up to 1000°C. For the upcoming researches, fillers already procured in high temperature could be used to avoid phase changes appearing in the material and resulting in microcracking of the structure.

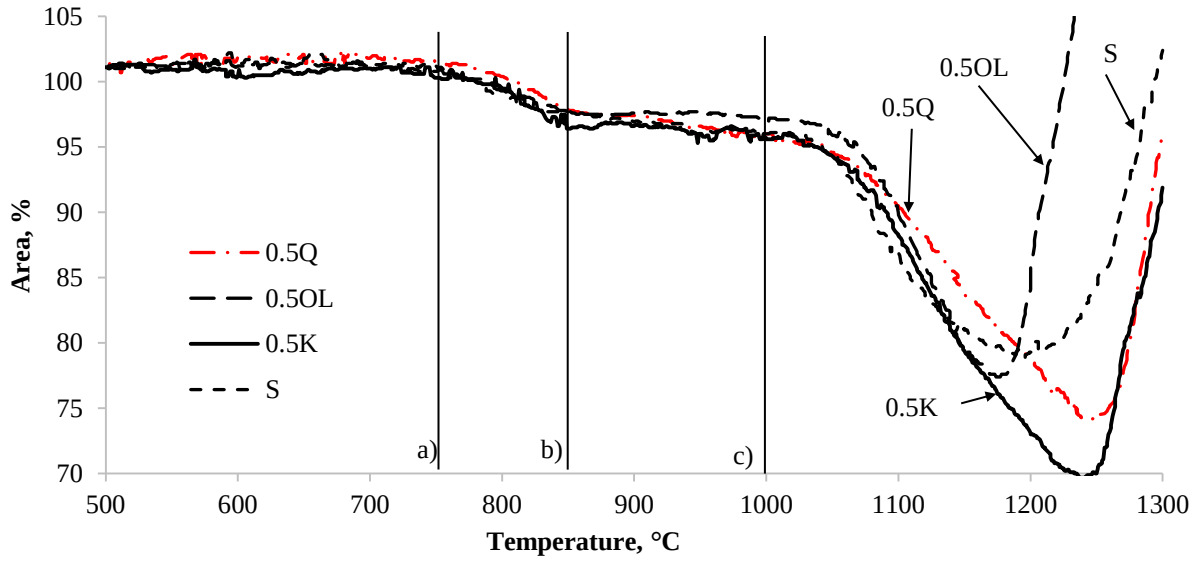

Figure 9. High temperature microscopy curves: relative area change of AAM during the heating.

4. Conclusions

Results indicate that the porous alkali activated materials (AAM) with quartz, olivine sand and firebrick by-product fillers could be obtained with density of 600 to 880 kg/m^3. It can be concluded, that the main impact of the material strength characteristics derives from the material structure determined by the

fineness of filler. The compressive strength of the prepared AAM was in the range of 0.8 to 2.0 MPa, however it changed during the heat treatment. For the AAM with the firebrick filler K26 the strength results increased up to 2.7 MPa and in flexural strength – up to 1.0 MPa. Strength properties of the AAM with K26 microfiller remained unchanged even after the temperature exposure of 1000°C. Strength decreased in the rest of samples. The microstructure of AAM could be damaged due to the filler expansion and zeolite crystal melting and transformation. Dimensional shrinkage of materials is observed within temperature interval of 750°C to 780°C, compiling the max shrinkage around 4% of the total area in all of the series of samples. It is concluded, that up to 1000°C the fillers (quartz, olivine sand and K26) used in this study have no significant influence on the heat resistance of AAM and their shrinkage.

Acknowledgements
This study was partially funded by the Riga Technical University under the project 34-24000-DOK.BIF/16.

References
[1] Gartner E 2004 Industrially interesting approaches to low-CO2 cements *Cem. Concr. Res.* **34** 1489–1498
[2] Zhang H Y, Kodur V, Qi S L, Cao L and Wu B 2014 Development of metakaoline-fly ash based geopolymers for fire resistance applications *Constr. Build. Mater.* **55** 38–45
[3] Lemougna P N, MacKenzie K J D and Melo U F C 2011 Synthesis and thermal properties of inorganic polymers (geopolymers) for structural and refractory applications from volcanic ash *Ceram. Int.* **37** 3011–3018
[4] Rickard W D A, Vickers L and Van Riessen A 2013 Performance of fibre reinforced, low density metakaolin geopolymers under simulated fire conditions *Appl. Clay Sci.*
[5] Vickers L, Rickard W D A and Van Riessen A 2014 Strategies to control the high temperature shrinkage of fly ash based geopolymers *Thermochim. Acta*
[6] Kamseu E, Rizzuti A and Leonelli C 2010 Enhanced thermal stability in K2O-metakaolin-based geopolymer concretes by Al2O3 and SiO2 fillers addition *J. Mater. Sci.* **45** 1715–1724
[7] Lorber K E and Antrekowitsch H Treatment and disposal of residues from aluminium dross recovery
[8] Zhang Z, Wang H, Provis J L, Bullen F and Reid A 2012 Quantitative kinetic and structural analysis of geopolymers. Part 1. The activation of metakaolin with sodium hydroxide *Thermochim. Acta* **539** 23–33
[9] Jacobs P A 1984 Structure and reactivity of modified zeolites *Proceed. of an int. conf. Prague*
[10] Benboudjema F, Guillon E and Torrenti J 2002 Effect of interfacial transition zone and aggregates on the time- dependent behavior of mortar and concrete